

Mechanical and Microstructural Investigation of Novel Bio-Inspired DNA and Hybrid Lattices

CHOUHAN, Ganesh, BORADE, Himanshu, YADUWANSI, Deepak Kumar, ESSA, Khamis and BIDARE, Prveen

Available from Sheffield Hallam University Research Archive (SHURA) at:

<https://shura.shu.ac.uk/36017/>

This document is the Accepted Version [AM]

Citation:

CHOUHAN, Ganesh, BORADE, Himanshu, YADUWANSI, Deepak Kumar, ESSA, Khamis and BIDARE, Prveen (2025). Mechanical and Microstructural Investigation of Novel Bio-Inspired DNA and Hybrid Lattices. Proceedings of the Institution of Mechanical Engineers, Part L: Journal of Materials: Design and Applications. [Article]

Copyright and re-use policy

See <http://shura.shu.ac.uk/information.html>

Mechanical and Microstructural Investigation of Novel Bio-Inspired DNA and Hybrid Lattices

Ganesh Chouhan¹, Himanshu Borade², Deepak Kumar Yaduwanshi³, Khamis Essa⁴, Prveen Bidare^{5*}

^{1,2,3}Department of Mechanical Engineering, Medi-Caps University, Indore 453331, India.

⁴School of Mechanical Engineering, University of Birmingham, Birmingham, B15 2TT, UK

⁵School of Engineering and Built Environment, Sheffield Hallam University, Sheffield S1 1WB, UK

Abstract

Additive manufacturing is transforming structural design for industrial applications by enabling the fabrication of complex, biologically inspired geometries with high precision. This approach enhances mechanical performance by maximizing strength and minimizing weight, paving the way for next-generation lightweight, high-strength structures. This study investigates bioinspired designs based on natural elements such as DNA, the nautilus shell, and the basal body. Two structures, a DNA-based and a hybrid design, were additively manufactured and analysed, incorporating variations in wall thickness (0.8 mm and 0.9 mm), DNA patterns (hexagonal and single), centriole-inspired tube angles (35° and 40°), and three curvature configurations in the nautilus structure. Mechanical performance was evaluated through both numerical simulations and experimental testing, and results were compared with earlier designs (centriole, nautilus, and hybrid). The hexagonal DNA structure posed manufacturability challenges due to its intricate fine links. However, components produced via the Vat Photopolymerization process exhibited excellent strength-to-weight ratios, combining lightweight properties with structural integrity. Compressive strength and failure mechanisms were also analysed, showing superior stiffness and energy absorption. Remarkably, the DNA and hybrid structures matched the strength of conventional designs while reducing material usage by approximately 45% and 25%, respectively. Additionally, microstructural analysis of the fractured surfaces provided insight into failure modes and post-deformation material behaviour.

Keywords: Bioinspired, DNA, compressive strength, additive manufacturing, lightweight.

1. Introduction

The development of bioinspired structures that not only resemble conventional designs but also surpass them in performance has long been a focal point of research and engineering efforts. Various species, including both flora and fauna, provide engineers and scientists with valuable opportunities to analyse their structural patterns, material composition, and functional performance under extreme environmental conditions. Bioinspired structures have recently emerged as a prominent focus in research due to their remarkable mechanical properties and functional advantages [1]. The development of advanced, lightweight natural biological materials [2] is crucial for applications necessitating enhanced energy absorption capabilities [3], particularly in sectors including transportation, aviation, and infrastructure. Nevertheless, strength and stiffness are frequently compromised in the lightweight design of lattice. Drawing inspiration from various biological systems, including the Centriole, Nautilus, the Cartwheel, and DNA, bioinspired structures demonstrate substantial advancements over conventional lightweight structures.

Bioinspired structures derive design principles from nature, leading to innovative, efficient, and sustainable solutions in engineering, architecture, and materials science. By analysing the adaptive strategies of diverse organisms, designers can develop structures that are not only aesthetically refined but also precisely optimized for performance and resource efficiency. Various bio-inspired structures serve diverse applications. For instance, 3D-printed hybrid lattice structures are designed for energy absorption, making them ideal for applications such as footwear and impact protection. Various bio-inspired structures serve diverse applications. For instance, 3D-printed hybrid lattice structures are designed for energy absorption, making them ideal for applications such as footwear and impact protection [4] and 3d printed elytra-like interlocked sandwich (ABEIS) structure used for excellent mechanical performance and energy absorption suitable for the applications in industries where lightweight yet strong materials are required, such as aerospace and automotive engineering [5].

Bionic lattice structures pomelo peel can be utilized in innovative structural designs that require materials with enhanced mechanical characteristics and energy absorption behaviours, making them suitable for applications in protective gear, automotive components, and aerospace structures[6, 7]. Metallic samples constructed from triply periodic minimal surfaces (TPMS) and cage lattices are designed for lightweight applications to use in aerospace and automotive engineering [8, 9].

Ramakrishnan et al. [10] worked on a bio-inspired Xylotus lattice, demonstrated for superior energy absorption characteristics, exceeding previous studies by a remarkable 38%. Zengmiao et al. presented a bio-mimetic curved-elliptical lattice configuration that significantly augments mechanical efficacy and deformation resilience [11]. Edoardo Mancini et al. [12] developed a bi-linear material using Digital Light Processing (DLP) technology, demonstrating isotropic behavior within a specific range of relative density at both meso and macro scales. Masoud Shirzad et al. [13] examined bioinspired auxetic structures under static and dynamic loads, concluding their potential for biomedical applications due to their tissue-like properties, enhanced durability, and superior energy absorption.

The present research introduces a novel structural design approach that uniquely hybridizes DNA, centriole, and nautilus-inspired geometries to create architected lattices for mechanical characterization. Unlike existing lattice frameworks such as TPMS or auxetic structures, the proposed designs exhibit hierarchical and multiscale features that have not been previously explored. This study aims to evaluate both experimental and numerical performance of these structures in terms of energy absorption, stiffness-to-weight ratio, and manufacturability using SLA-based 3D printing. While TPMS structures are known for their high surface-to-volume ratio and mechanical efficiency [14], and auxetic lattices for their negative Poisson's ratio and enhanced energy absorption [15], our hybrid structures offer a distinct alternative by integrating biological inspiration from multiple natural forms, potentially offering superior performance in lightweight applications. Hybrid lattice structures can effectively balance performance trade-offs by combining the strengths of different geometries. AlQaydi et al. [16] demonstrated that while I-WP lattices delivered superior stiffness along the build direction, they also exhibited pronounced anisotropy. In contrast, diamond lattices showed more uniform mechanical behavior but with comparatively lower stiffness, emphasizing the challenge of optimizing both strength and directional stability. Limited studies have explored the constitutive behaviour of hybrid lattice structures [17–19]. Di Frisco et al. [20]. demonstrated that topological modifications in TPMS lattice designs can significantly enhance the mechanical performance of integrated structures, achieving up to a fourfold increase in energy absorption.

The intricate structure of deoxyribonucleic acid (DNA), from the nucleotide level to the chromosomal scale, is fundamental to its biological function. DNA's capacity to store and transmit genetic information effectively is intrinsically linked to the sophistication of its structural design. DNA serves as the fundamental genetic blueprint for humans and nearly all living organisms. Remarkably, the DNA within almost every cell of an individual's body

remains identical, ensuring consistency in genetic information. DNA sequences are delivered from parent to baby, with the father's DNA responsible for around half of a child's DNA and the mothers for the other half. A series of nucleotides makes up a DNA molecule. Three basic building blocks make up each nucleotide: a nitrogenous base, a phosphate group, and a sugar molecule. The cell's nucleus contains the majority of the DNA; however, the mitochondria also contain a little. The four chemical bases that make up DNA's coding (T) are adenine (A), guanine (G), cytosine (C), and thymine (T) [21, 22]. The DNA structure is remarkably precise, maintaining a uniform width, consistent nucleotide spacing, and a well-regulated length. Each helix turn follows a strict pattern, ensuring stability and integrity at the molecular level.

The 3D structure of a DNA molecule forms an elegant right-handed double helix, where hydrogen-bonded bases stack atop one another, oriented perpendicular to the sugar-phosphate backbone. Along the helical axis, these bases are precisely spaced at 0.34 nm intervals. With each complete turn occurring every 3.4 nm, the helix elegantly accommodates approximately 10 base pairs per rotation, ensuring its stability and functionality [23]. DNA boasts a precisely structured helical width of 2.0 nm, with each base pair contributing to a graceful +36-degree rotation, creating its iconic spiral symmetry [24]. The number of DNA is selected six because simulation results in better strength than 2 and 4 DNA.

This study builds upon previous research by introducing two novel nature-inspired designs (DNA and Hybrid) and comparing them with existing structures (Centriole, Nautilus, and Hybrid) [1]. The preliminary design and development were carried out using SLA-based additive manufacturing, supported by numerical simulations to predict the mechanical performance of the new lattice geometries. Subsequently, a comprehensive experimental campaign was conducted to evaluate the static mechanical properties of the structures across varying wall thicknesses and to investigate their deformation mechanisms under uniaxial compression. The study also presents the design development approach, along with the validation of physical and numerical deformation points. Finally, fracture surface morphology was examined using scanning electron microscopy (SEM) to gain insights into failure characteristics and microstructural behaviour.

2. Material and Methods

This study builds upon our previous research by investigating optimized design strategies for homogeneous bioinspired DNA-based lattices and hybrid structures. We also compare these designs with structures such as the centriole, nautilus, and cartwheel, which were analysed in the earlier publication[1]. This study introduces a novel hybrid structure that integrates

elements of the centriole, nautilus, cartwheel, and DNA architectures. The CAD model was meticulously designed using Autodesk Fusion 360, showcasing a robust 50 mm diameter and an equal height of 50 mm for structural consistency and precision.

2.1 DNA Structure Design

Drawing inspiration from the natural DNA double helix, the design preserves a base pair diameter of 2 mm, aligned with a sequence of 10 base pairs. The axial distance between successive base pairs is uniformly scaled to 3.04 mm, creating nine intermediate gaps that reflect the helical pitch. To ensure structural integrity and balance between the rib structure and the top plate, the backbone diameter is set at 5 mm for both single and double-strand configurations (See Figure 1). The entire geometry is derived through a dimensional upscaling from molecular scale to printable form, adopting a transformation ratio of 1 nanometre to 1 millimetre. The overall height of the single and double DNA structures corresponds to one complete helical cycle, scaled from 3.4 nm in the natural molecule to 48 mm in the fabricated design. In the case of the hexagonal DNA configuration, the combined diameter of all six helices spans approximately 48 mm, effectively occupying the entire 50 mm diameter of the build plate. The diameter of each DNA diameter is 8mm. To maintain geometric proportionality, the height of the hex DNA structure is adjusted to include two complete cycles, resulting in a total height of 48 mm (with each cycle scaled to 24 mm). For the hexagonal DNA structure, the backbone diameter was set to 0.815 mm. This value was derived by proportionally dividing the 5 mm backbone diameter used in the single DNA configuration across six helices, resulting in a reduced yet structurally consistent dimension. Similarly, the base pair diameter was downscaled from 3.04 mm to 0.5 mm to fit the compact hexagonal arrangement. This scaling ensures that the collective geometry fits within the design constraints while maintaining mechanical stability.

Table 1 illustrates that designs D1 and D3 employ the smaller 8 mm diameter, whilst designs D2 and D4 utilize the larger 48 mm diameter. The mass of each design was evaluated using slicing software. The hexagonal DNA structure with a backbone thickness of 0.8 mm weighs approximately 18.5 g, while the single DNA configuration has a mass of 21.1 g. This difference underscores the influence of structural density and the number of DNA units on the overall weight. The dual DNA structure exhibits the highest mass at 31.24 g, an increase of nearly 33% compared to the single DNA due to the added helical strand and increased material volume. This variant facilitates the optimization of mechanical qualities according to design specifications. Despite the relevance of their complex geometry, current hexagonal DNA nanostructures face challenges during the printing process, notably the structural failure of

thinner rib sections. In contrast, such issues are not observed in single DNA lattice configurations, indicating superior mechanical stability in simpler architectures.

Table 1 DNA structures design variables

Variables	D ₁	D ₂	D ₃	D ₄
Individual Units	6	6	1	1
Mass	18.5 g	20.6g	21.1 g	22.3 g

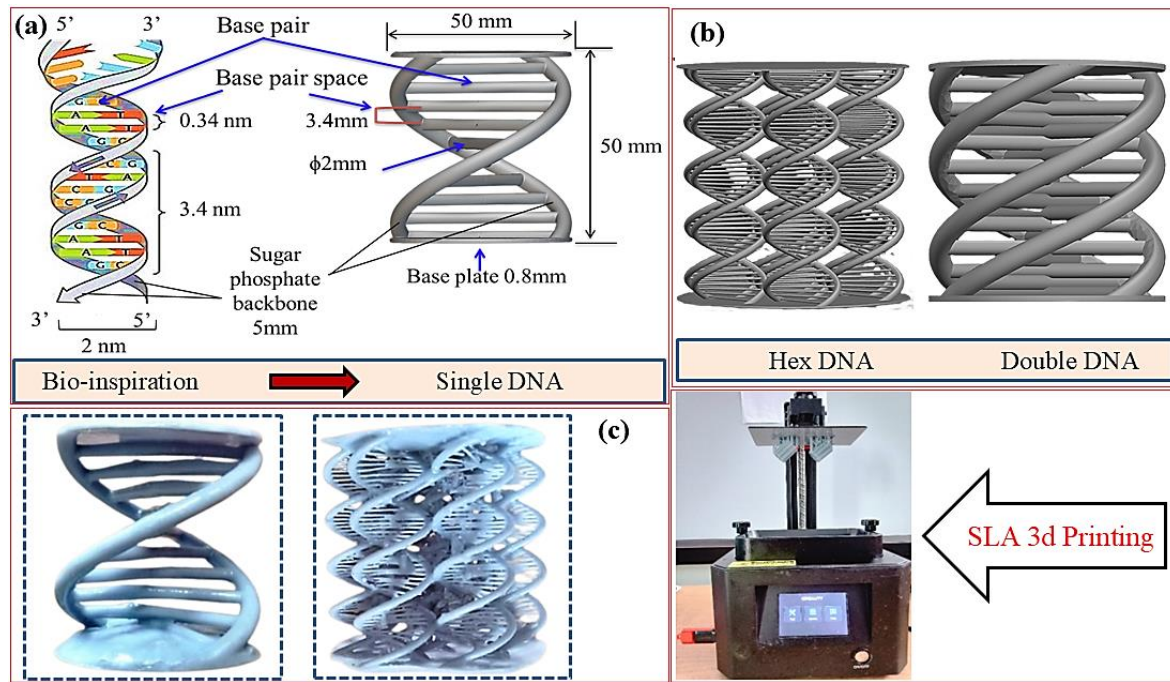


Figure 1 a) DNA structure of sugar-phosphate backbone[25], b) Hex and single DNA design, and b) SLA printed samples.

2.2. Hybrid [Centriole + Nautilus+ DNA] Structure Design

The hybrid structure integrates elements of centriole, nautilus, and DNA architectures. Single and hex DNA are selected based on simulation results. The selection strategy for the two hybrid lattice designs involves deliberate variation in the height combinations of DNA (half-cycle and full-cycle) and centriole elements to achieve distinct structural responses. In Design A, the hex DNA height is reduced from its original 48 mm to 24 mm (based on the hex DNA configuration) and is combined with a 26 mm spiral centriole, distributed as 13 mm on the top and bottom sections (see Figure 2). This arrangement emphasizes enhanced vertical support from the centriole structure while maintaining a compact DNA core.

In contrast, Design B incorporates a halved single DNA unit with a height of 24 mm (derived from the full 48 mm single DNA design), paired with the same 26 mm spiral centriole. This configuration leverages the DNA's helical characteristics, potentially enhancing torsional

flexibility and energy absorption. The half single DNA structure contains 5 base pairs, each with a diameter of 2 mm, spaced consistently at 3.04 mm, and supported by a 5 mm diameter backbone preserving the original geometric parameters of the full DNA model. These design modifications provide customized mechanical properties and functional versatility based on the specific use of the hybrid lattice structure.

Table 2 Hybrid structures design variables

Variable	H ₁	H ₂	H ₃	H ₄
Thickness of Wall (in mm)	0.8	0.9	0.8	0.9
Tube Angle (degrees)	40	40	35	35
No. of curves	3	3	4	4
Individual Units of DNA	6	6	1	1
Mass (grams)	23.6	24.2	23.8	24.3

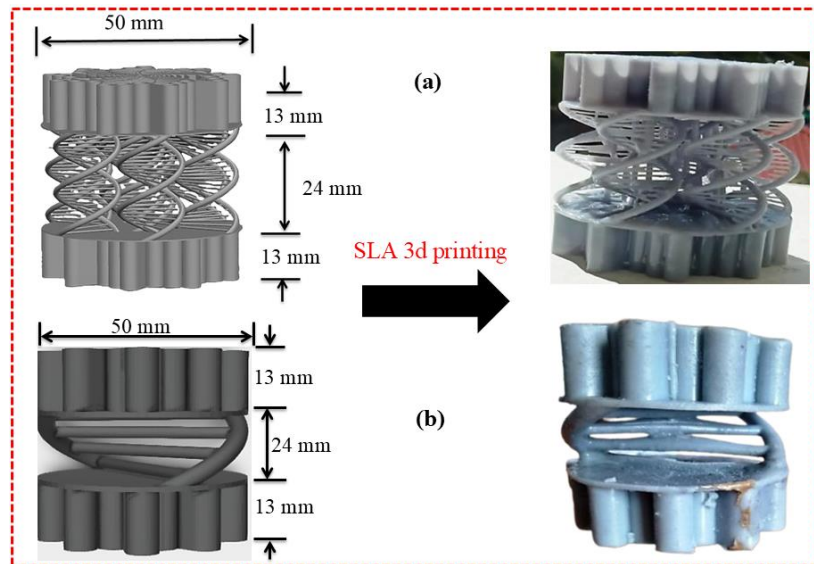


Figure 2 Dimension of the Hybrid designs a) Designs of hex and Single Hybrid lattice and b) Printed Part of hex and single hybrid lattice structure.

2.3 Additive Manufacturing Samples

As illustrated in the design above, two primary geometric shapes with nine distinct lattice configurations were fabricated using advanced stereolithography (SLA) techniques. The structures were crafted from elegoo ABS standard photopolymer resin (405 nm), renowned for its exceptional precision, minimal volume shrinkage (3.72-4.24%), impressive tensile strength (30-52 MPa), and optimal density (1.05-1.25 g/cm³), ensuring robustness and accuracy in the final constructs. Creality LD002R 3D printer, with a compact yet efficient build volume of 119 x 65 x 160 mm, operates at a variable print speed of 6-18 seconds per layer height and a nominal power consumption of 72W. Beyond precise fabrication, this machine also calculates essential metrics such as part volume, mass, estimated print time, and cost analysis. The SLA printing

settings are established as follows: the layer height is 0.05 mm, assuring fine detail and an ideal surface finish. Each layer necessitates an exposure time of 7 seconds; however, the lower layers demand an extended exposure period of 60 seconds to enhance adherence to the construction plate. The bottom lift distance is established at 5 mm, accompanied by a bottom lift speed of 65 mm per minute. The retraction speed is set at 150 mm per minute to enhance print efficiency and minimize possible defects. The steps to develop and testing of all bio-inspired lattices is explained in Figure 3. All samples were printed in a flat orientation to ensure dimensional consistency and reduce potential warping during the SLA printing process. The single DNA structures required minimal support, as their geometry was relatively self-supporting. In contrast, the hybrid structures demanded additional support, particularly to stabilize the overhanging plates and interconnected features during the build process. For the hexagonal DNA structures, thin supports were strategically placed to maintain fine feature resolution while minimizing post-processing challenges. After printing, all structures were cleaned using isopropyl alcohol which effectively removes residual uncured resin, preventing sticky surfaces and enhancing surface finish. Incomplete washing may lead to resin pooling, which can harden unevenly during post-curing, negatively impacting both the aesthetic quality and mechanical integrity of the part. Post-curing under UV light further increases the degree of polymer crosslinking, leading to improved stiffness, strength, and hardness. Without adequate curing, parts may remain undercured, brittle, and mechanically compromised. post-cured under a 405 nm UV light source to enhance material strength and stability.

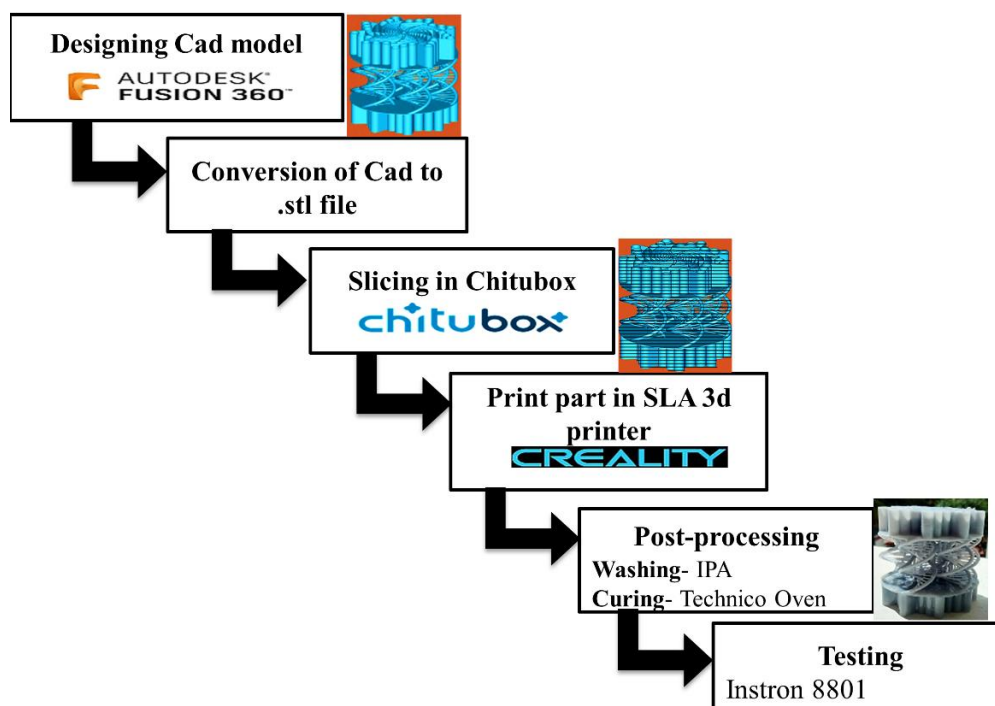


Figure 3 Standard procedure for developing the bioinspired structure.

The density of each of the five biological samples can be precisely determined by the below formula:

$$\rho = \frac{m}{v} \quad 1)$$

Based on the above values, the liquid density is maintained at 1.1 g/cm³. Table 3 reports experimentally determined densities of DNA and hybrid structures, benchmarked against previously reported values for three bioinspired lattices—centriole, cartwheel, and nautilus. Average densities from five samples per geometry were normalized to the base photopolymer resin.

Table 3 Experimental relative density of bio-inspired samples

Structure	Centriole	DNA	Nautilus	Cartwheel	Hybrid
Density (g/cm ³)	0.9838	0.9863	0.9922	0.9848	0.9866
Relative Density	0.8943	0.8966	0.902	0.8952	0.8969

$$\text{Relative density} = \frac{\rho_{\text{sample}}}{\rho_{\text{solid}}} \quad 2)$$

The hardened conventional gray resin possesses a density of 0.98 g/cm³. Even though the mean relative density is 10.2% less, the measured densities are remarkably accurate and closely match the expected values. This discrepancy, which may be connected to the loss of liquid resin while producing finer designs like the centriole and nautilus, highlights the challenges associated with high-precision 3D printing.

During the fabrication process using SLA 3D printing, we observed a failure rate of approximately 18%, primarily associated with the DNA-hexagonal structures. These failures were due to fragile interconnections, unsupported overhangs, and delamination during post-curing. To overcome the failure rate and improve manufacturability, several key factors should be considered. One of the most effective strategies is design optimization, which includes thickening critical connections and introducing supportive ribs in regions prone to failure to enhance structural stability during printing. Additionally, the strategic placement of custom or denser support structures is essential for minimizing deformation and ensuring dimensional accuracy. Furthermore, reducing UV post-curing intensity or duration can help prevent cracking, particularly in fine-featured areas and thin-walled sections, where excessive curing may lead to brittleness or delamination.

2.4 Development of the Lattice

The development of DNA and hybrid bioinspired structures is systematically divided into five phases of printing utilizing nTopology software. The initial phase of DNA construction involves the building of a base plate to ensure a stable foundation. This is succeeded by the incremental printing of the DNA strands in backbones, signifying the intermediate stages where

the distinctive helical characteristics materialize. The structure is finalized with a top plate, guaranteeing general stability and symmetry. The hybrid design commences with a cartwheel design in the lower layers that emulates natural support systems, succeeded by the development of a solid plate. This is subsequently overlaid with a DNA structure at the center, succeeded by another plate, and ultimately reverts to the cartwheel pattern at the apex.

A single DNA structure has two backbones, whereas a dual DNA structure has four, adding another level of complexity to the manufacturing process. The DNA type determines the design complexity. In the case of dual DNA designs, the gap between the ribs is either completely absent or very small. This leads to premature deformation under load, resulting in an undesirable aesthetic for the design. Conversely, hexagonal DNA molecules has exceedingly thinner ribs, rendering precise printing challenging. Despite their susceptibility to rapid fracture under mechanical stress, these slender ribs have the benefit of enhanced energy absorption, essential for applications demanding impact resistance and force dissipation.

Figure 4 depicts the developmental phases of the proposed lattice structure, emphasizing the progression of geometric patterns during the design process. Each step signifies a unique configuration in which the spatial arrangement of elements such as DNA-inspired helices, centriole spirals, and cross-links experiences gradual refinement. These steps illustrate how the amalgamation of various components affects the overall structural configuration, symmetry, and connection. Initial phases may reveal simpler, more open structures, whereas subsequent phases demonstrate heightened complexity and structural density, indicating the shift from conceptual design to a more functionally efficient lattice.



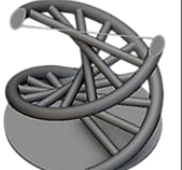





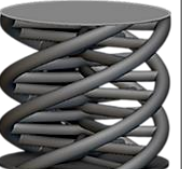


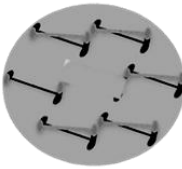
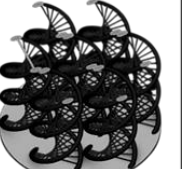
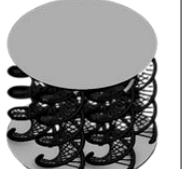


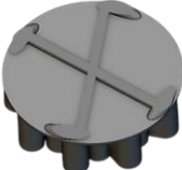


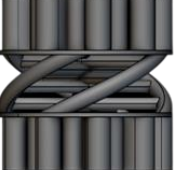

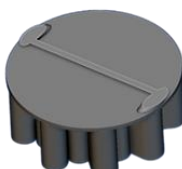


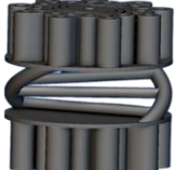

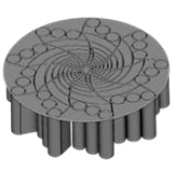
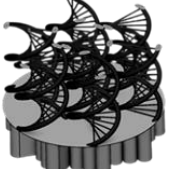
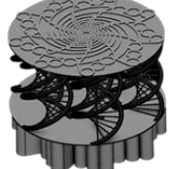
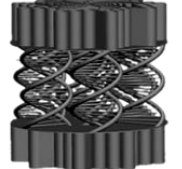
Initial Layers (Bottom Plate)	Middle Layers (Formation of 1DNA Backbones)	Middle Layers (Addition of DNA Backbones)	Top Layers (Top Plate)	Final Single Design
				
Initial Layers (Bottom Plate)	Middle Layers (Formation of 2DNA Backbones)	Middle Layers (Addition of 2DNA Backbones)	Top Layers (Top Plate)	Final Double DNA Design
				
Initial Layers (Bottom Plate)	Middle Layers (Formation of 6DNA Backbones)	Middle Layers (Addition of DNA Backbones)	Top Layers (Top Plate)	Final Single Design
				
Initial Layers (Bottom phase of Cartwheel)	Middle Layers (Formation of 2 DNA Backbones)	Middle Layers (Addition of DNA Backbones)	Top Layers (Top phase of Cartwheel)	Final Hybrid Design
				
Initial Layers (Bottom phase of Cartwheel)	Middle Layers (Formation of 1 DNA Backbones)	Middle Layers (Addition of DNA Backbones)	Top Layers (Top phase of Cartwheel)	Final Hybrid Design
				
Initial Layers (Bottom phase of Cartwheel)	Middle Layers (Formation of 6 DNA Backbones)	Middle Layers (Addition of DNA Backbones)	Top Layers (Top phase of Cartwheel)	Final Hybrid Design
				

Figure 4 Schematic diagram of the Development stages of lattices

2.5 Experimental Testing

Figure 5 presents the quasi-static test setup, the samples evaluated, and the resulting performance outcomes for the selected DNA and hybrid structures. A total of nine samples

were tested: five samples from the DNA-based structures including single, hexagonal, and dual configurations with 0.8 mm and 0.9 mm thicknesses, and four samples from the hybrid lattice structures in single and hexagonal forms, also with 0.8 mm and 0.9 mm thicknesses. The samples were put through a compression test utilising the Instron 8801 material strength measurement equipment, which has a hydraulic pressure supply of 207 bar, an actuator stroke of 150 mm, and a load capacity of 100 kN. With an initial displacement rate of 1.5 mm/min, the test was carried out at room temperature with precise control using wave matrix-2 dynamic testing software.

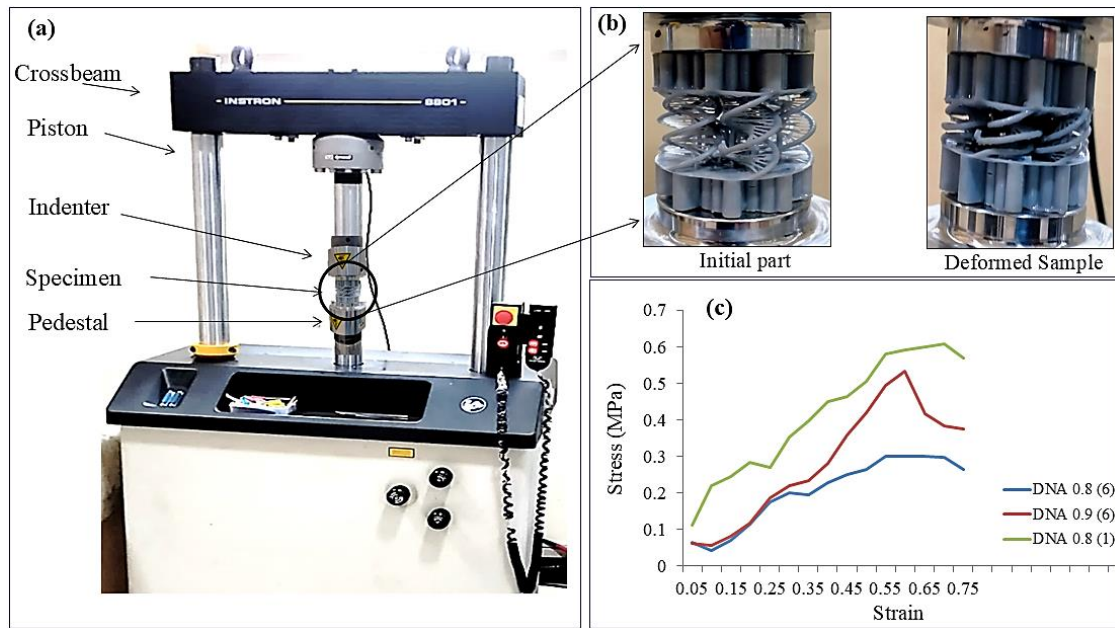


Figure 5 Testing procedure and results: a) Testing facility-Instron 8801, b) deformation pattern and c) graphical results-stress-strain curve.

The identical loading procedure was used for all specimens to prevent the build print pattern from affecting the mechanical behaviour. When the power dropped by 80%, just below the maximum force, or when the reaction force hit 20 kN, the compressive testing was terminated. The printed part's maximum loading capacity is indicated by this value. Stress-strain curves are used to test and document the deformation behaviour of every component. Elegoo abs standard photopolymer resin specimens are mechanically brittle, shattering under high stress at tiny stresses.

2.6 Simulation Framework

The ANSYS simulation was designed to closely replicate the experimental compression test conditions by applying appropriate boundary constraints. The bottom surface of the lattice structure was fully fixed, while the top surface was subjected to a constant downward velocity of 2 mm/s, simulating the compression loading. It was assumed that the top boundary had no

lateral or longitudinal displacements, thereby restricting any unintended movement during deformation. For both experimental and numerical analysis, a 100 kN load capacity was considered. Each lattice structure was meshed using a refined finite element (FE) mesh, with further mesh refinement applied to accurately capture stress distribution, particularly the von Mises stress. The smallest element size ranged from 0.25 to 0.5 mm, resulting in 246,579 mixed elements and 73,937 nodes in the final mesh.

3. Results and Discussion

3.1 Deformation Patterns

Figure 6 shows the deformation pattern for several bio-inspired lattice designs. It is evident that each has a unique lattice deformation mode. The deformations of the parts at different strain degrees of $\varepsilon = 0\%$, 20%, 30%, 55%, and 75%. It is observed that all the designs reflect plastic deformation nature. The deformation pattern for single DNA structure starts from centre to top. The deformation from the centre occurs primarily due to the high number of base pairs, which, under increased load, come into contact and subsequently break. Furthermore, the DNA-based structure's backbone is gradually compressed until it hits a critical load limit, at which the structural collapse starts. The cracking is likely caused by the material's brittle characteristics, which do not provide adequate ductility to withstand additional stress. As compression intensifies, the backbone elements are inclined to bend outward from the central axis, so generating tensile forces perpendicular to the initial compression direction.

Initially, upon the application of compressive force, the cross-links converge, and during this phase, the structure has ductile behavior marked by elongation and energy absorption. Upon contact of the cross-links, the structure shifts from ductile deformation to brittle fracture. The core cross-links, crucial for stability, start to deform under the influence of axial compression and lateral tensile pressures. This localized distortion subsequently ascends, progressively undermining the top sections of the structure and resulting in a cascade failure mechanism. However, hex DNA shown sequential collapse due to lean structure and elastic behaviour up to one limit. Further observation of the hybrid structure's deformation reveals that energy absorption occurs initially, followed by the fracture initiation in the base pair, extending towards the upper and lower centriole sections.

The two-boned hybrid construction has grown somewhat heavy and dense in comparison to other bio-inspired structures. Completely brittle behaviour is displayed by printed parts, with all samples failing at low strain levels. The sample presents elastic-plastic deformation pattern. However, hybrid tested parts show higher compressive strength. Deformation patterns for

different shorts of DNA (Hex, double and single) lattice structures are different. The different elastic stiffness of the structure is the reason for the different collapse patterns. Changing the number of vertical chains is also an option. The number of ribs is proportional to the number of chains and is a key component in enhancing energy absorption. Although the backbone diameter has been enlarged, it does not exceed the maximum allowable. Increased backbone diameter can lead to increased strength and weight, as well as decreased energy absorption. The hex DNA structure is very lean and complex. The energy absorption behaviour is excellent for Hex DNA (0.8).

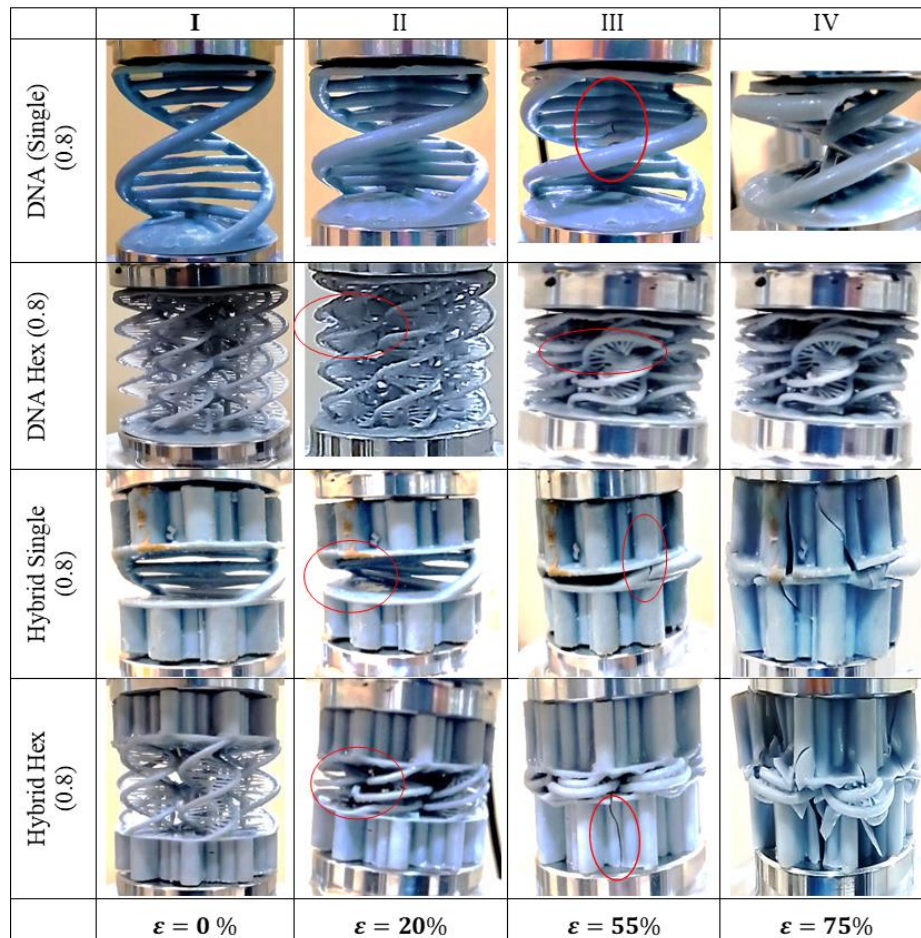


Figure 6 Failure patterns of all DNA and hybrid samples.

3.2 Stress-Strain Response

In order to evaluate the disparity in mechanical properties among various DNA and hybrid lattice structures, quasi-static testing was conducted on structures of identical size. The structural design of lattices has a major impact on their stiffness, compressive strength, and load-bearing capacity, as demonstrated by Figure 7. The DNA 0.8 Hex lattice exhibited the lowest performance, with a maximum compressive load of 0.592 kN, modulus of 0.45866 MPa, and compressive strength of 0.3016 MPa, indicating a relatively flexible and less stiff structure. In comparison, the DNA 0.9 Hex lattice showed improved mechanical behavior, sustaining a

load of 0.732 kN with a modulus of 0.6752 MPa and compressive strength of 0.5341 MPa, suggesting that increased lattice density enhances resistance to compressive forces. The lower values observed for the hex DNA structure can be attributed to the presence of six backbones and the thin cross-sectional dimensions of the ribs.

The DNA 0.9 Single lattice further outperformed the hex variants, achieving 1.193 kN load capacity, a significantly higher modulus of 4.37767 MPa, and compressive strength of 0.6076 MPa, indicating greater structural integrity and stiffness. The DNA 0.8 Double lattice demonstrated the highest mechanical performance across all metrics, withstanding 1.362 kN, and exhibiting a modulus of 5.6842 MPa and compressive strength of 1.0453 MPa, reflecting its superior ability to resist deformation under compression due to its doubled strand design. These results collectively highlight that mechanical properties of DNA lattices improve with increased structural density and simplification, where higher modulus values correlate with increased compressive strength, emphasizing the role of architectural design in enhancing structural mechanics.

In accordance to the Figure 7 (a) illustrates the mechanical response of the DNA lattice system under three successive loading and recovery cycles. Each phase is marked by a distinct peak in stress, showing progressive improvements in stiffness and strength, beginning at approximately 0.29 MPa, increasing to 0.3 MPa, 0.46 MPa, and reaching a maximum of 0.6 MPa. The final peak occurs when the structure is nearly fully deformed, and all ribs have made contact and fractured against each other. These successive stress peaks reflect the material's capacity to recover and exhibit enhanced performance across cycles, highlighting a multi-phase strengthening mechanism inherent to the DNA lattice design. Unlike the single DNA curve, which shows multiple distinct loading-unloading cycles, the hybrid structure exhibits a more continuous and stable deformation behaviour without abrupt drops, indicating gradual energy absorption. The stress increases progressively and reaches a peak value of approximately 0.298 MPa at the highest strain. Throughout the deformation process, the hybrid structure maintains a relatively linear response with moderate fluctuations, implying better structural integrity and load distribution compared to the pure DNA configuration. The absence of sharp stress drops or recovery peaks suggests that the hybrid structure deforms more uniformly, with less localized failure. This behaviour indicates a more ductile-like energy dissipation, which can be advantageous in applications requiring consistent energy absorption and mechanical reliability.

However, Figure 7(b) demonstrates that the hybrid single lattice surpasses the hybrid hex construction in stiffness, demonstrating significantly more rigidity. The hybrid hex curve exhibits a delayed load-bearing behaviour, with a prolonged low-stress region in the early

stages of deformation. This indicates initial structural flexibility or delayed engagement of load-bearing elements due to the geometry and thin ribs. The stress gradually increases and peaks at around 4.22 MPa, after which a slight softening or plateau behaviour is observed, suggesting the onset of local buckling, densification, or damage to the ribs. In contrast, the Hybrid DNA lattice exhibits a significantly higher stress response, with a steep rise culminating in a peak stress of around 16.83 MPa. The sharp increase indicates superior load-bearing capability, likely due to an optimized geometry combining elements of multiple lattice designs. The curve is smoother and continuous, suggesting progressive collapse without abrupt failure, and greater resistance to deformation. This indicates the hybrid architecture promotes enhanced structural integrity, improved stiffness, and greater energy dissipation under loading.

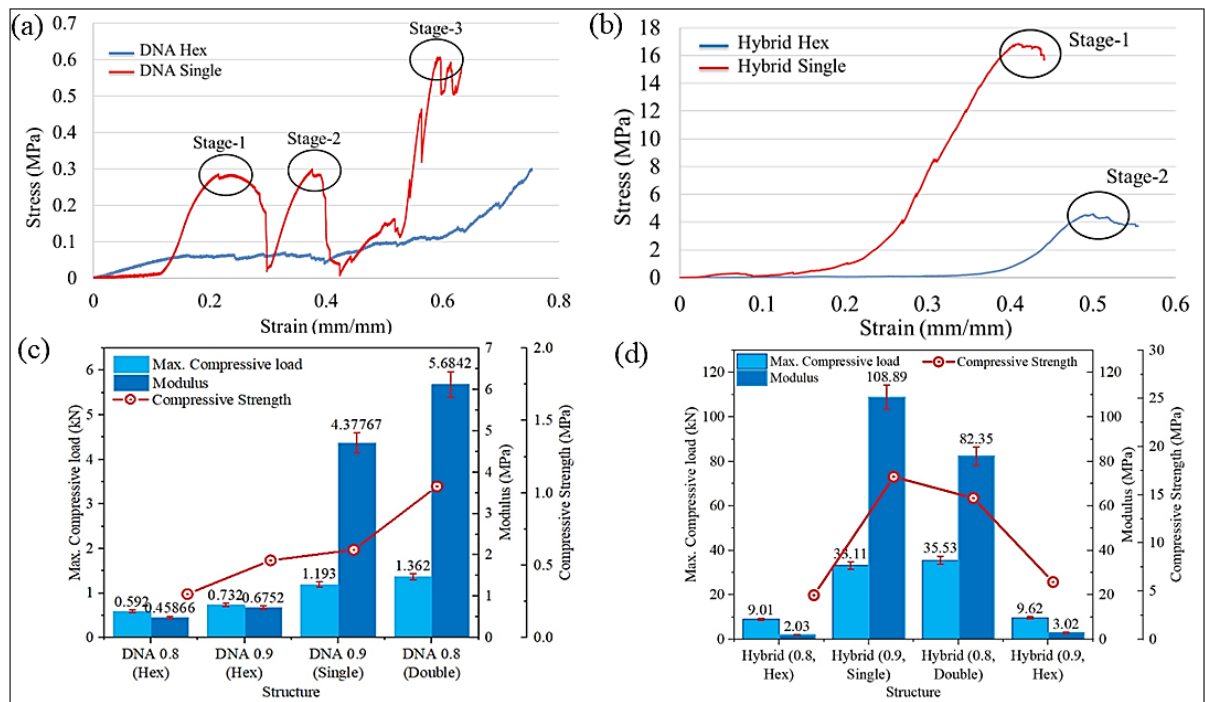


Figure 7 Stress-strain experimental results of different DNA structures.

The Hex DNA structures exhibit the lowest compressive strength (0.3016–0.5341 MPa), modulus (0.45866–0.6752 MPa), and load capacity (0.592–0.732 kN), primarily due to their thin ribs and limited connectivity. Transitioning to the Single DNA lattice significantly enhances stiffness (modulus 4.38 MPa) and load capacity (1.193 kN), while slightly improving strength (0.6076 MPa), indicating better structural integrity. The Double DNA structure demonstrates the best performance, with the highest compressive strength (1.0453 MPa), modulus (5.68 MPa), and load capacity (1.362 kN), attributed to its denser architecture and efficient load distribution. Overall, the results confirm that geometric design and scaling play a critical role in enhancing the mechanical behaviour of bio-inspired lattice systems. The hybrid structure exhibits elastic-plastic behaviour due to a combination of different structures.

Initially, the centre part DNA support to enhance the energy absorption up to the elastic limit and upper- and lower-part support to increase strength. The hybrid structure with hex DNA exhibits higher energy absorption and lower compressive strength. Moreover, Single DNA reflects higher strength with moderate energy absorption behaviour.

3.3 Simulation Results and Comparison

The comparative stress study of DNA-inspired and hybrid lattice structures reveals a significant disparity in mechanical performance (Figure 8). DNA-based structures demonstrated minimum von Mises stresses averaging 2.03 MPa and maximum stresses approximately 12.22 MPa, while hybrid lattices revealed considerably elevated values, with an average minimum stress of 7.97 MPa and a maximum stress of 57.38 MPa. This indicates an approximate 292% rise in lowest stress and a 370% rise in maximum stress in hybrid structures relative to DNA equivalents. Moreover, the internal stress amplification, as denoted by the percentage rise from minimum to maximum stress, exhibited significant variation across structures. DNA designs demonstrated increases between 394% and 756%, underscoring their ability for elastic deformation under stress. Conversely, hybrid lattices exhibited stress amplifications ranging from 551% to 755%, highlighting their enhanced load-bearing capacity attributed to increased nodal connectivity and structural densification. The findings highlight the promise of DNA-inspired designs for flexible applications necessitating high strain tolerance, whereas hybrid lattices are better suited for high-strength, load-bearing engineering structures.

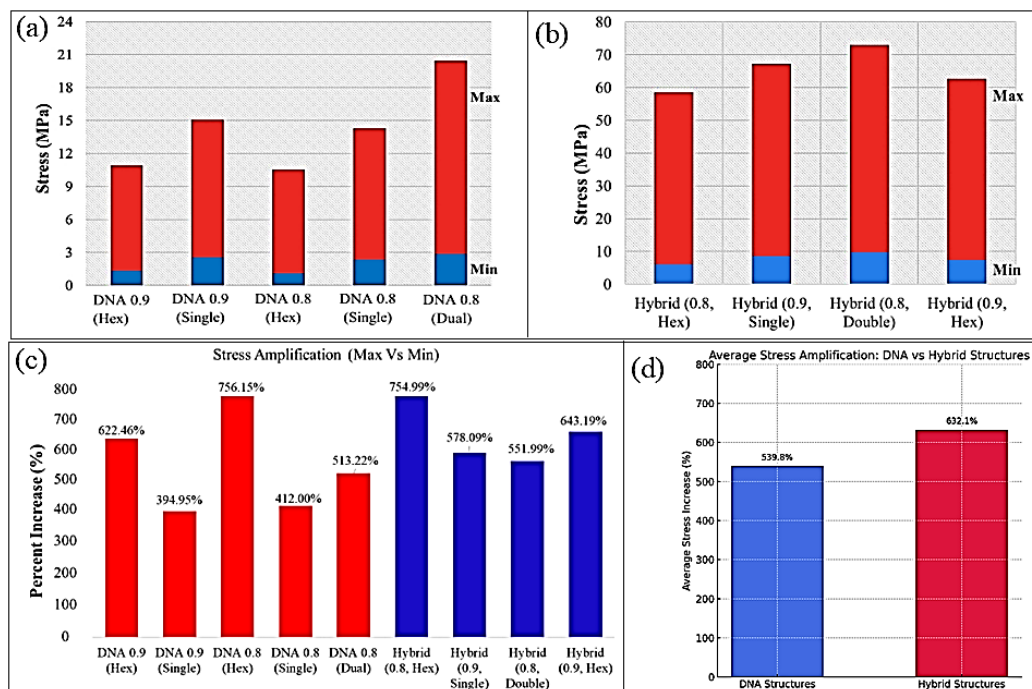


Figure 8 Von Mises stress of different Hybrid structures

The results in the corresponding Figure 9 demonstrate a strong relationship between simulation and experimental testing of the DNA lattice structure subjected to compressive load. The left side of the image displays a finite element analysis (FEA) illustrating the distribution of equivalent (von Mises) stress, with peak stress concentration located in the middle portion of the structure. This aligns well with the experimental image on the right side, where physical breakdown is evident. The deformation pattern indicates that under compressive loading, the backbone segments commence outward movement, producing tensile forces laterally. This external deflection not only causes bending in the cross-links but also exacerbates stress concentration at particular junctions. The simulation identifies the crucial high-stress region that confirmed by the physical test as the “first breaking zone” signifying the point at which the structure begins to disintegrate. The continued downward propagation of deformation leads to a "second breaking zone," thereby validating a cascading failure process. The congruence of high-stress areas in both simulations and experimental findings corroborates the precision of the computational model and reinforces the assertion that the interplay of compression-induced outward backbone deflection and lateral tensile forces substantially influences the fracture behavior of the structure.

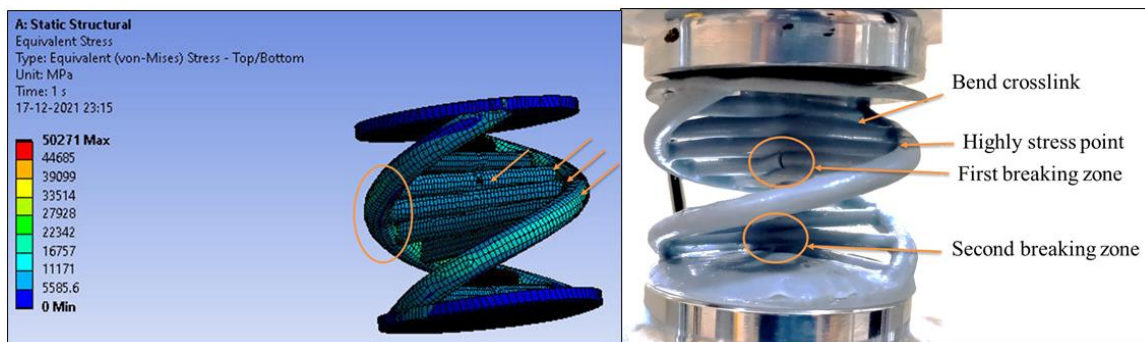


Figure 9 Numerical and physical testing validation

3.4 Influence of the Configurations of Hybrid Lattice

During the compression process, the maximum force of the hybrid structure was significantly higher than that of the other structures. The part's energy absorption capacity is provided by the DNA structure, while the cartwheel provides strength to sustain larger loads. Because of the larger helical diameter and connecting ribs, the single DNA is more suited for greater energy absorption. Individual centriole or nautilus shows 65% less energy absorption with rapid deformation. For thin size parts, centriole micro triplet tubes are suggested. Micro duplet cylinder is preferred for 0.9 thickness structures to keep the weight minimal. The nautilus structure acts as a support system in the hollow centre region of the centriole, preventing it from deforming prematurely.

The centriole structure, composed of interconnected tubes, resists axial and lateral loads, with mutual support enhancing overall strength and load capacity. Compared to hollow cylinders, it offers improved stress distribution and potential for use in cement-filled columns. Similarly, the nautilus curve design enables wide coverage without internal supports, reducing buckling and reinforcing both inner and outer surfaces. This geometry also enhances material efficiency, lowers costs, and ensures uniform axial load distribution with increased load-bearing performance.

3.2 Fracture Surface Analyses

3.2.1 Optical Microscopic View

The surface morphology of the deformed PLA specimens was examined to assess fracture behavior. All structures demonstrated characteristics consistent with brittle fracture, as evidenced by distinct cracking patterns, void formation, and the presence of melted particles and residual resin highlighted in the figures below. Crack initiation was commonly observed at the center of the structures, with propagation extending both upward and downward, indicative of rapid fracture with minimal plastic deformation. This behavior likely contributed to the observed reduction in mechanical strength of SLA-printed PLA specimens.

In the nautilus structure, layered fracture features were evident, while Figure 10 highlights the visual presence of voids. An increase in wall thickness from 0.8 mm to 0.9 mm corresponded with a rise in void density, suggesting a direct relationship between material accumulation and defect formation. Notably, buckle-type fractures were identified in the centriole and cartwheel structures, indicating localized structural failure under critical loading. The outer tubes of these structures exhibited bending deformation, forming strip-like geometries. Additionally, white shear zones were noted at crack tips in the centriole's outer tubes, while excess resin accumulation was prominently visible on both the nautilus and cartwheel geometries.

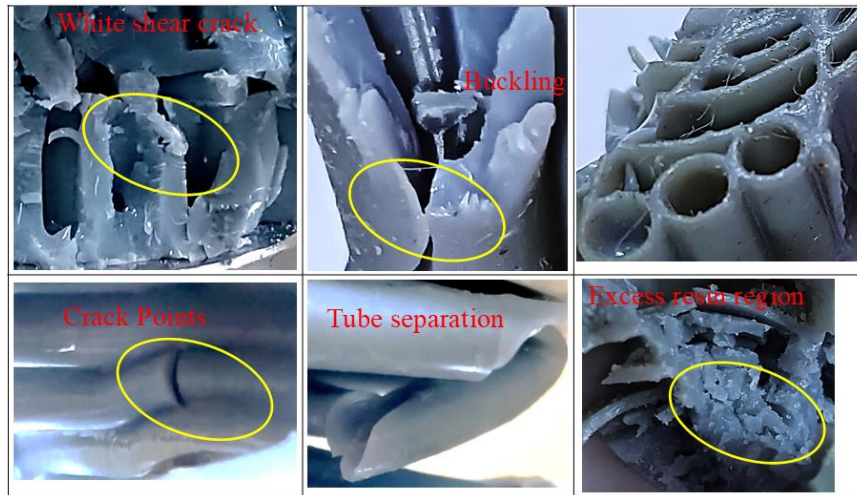


Figure 10 PLA fractured surface after testing.

3.2.2 Microscopic View

The SEM micrographs of fractured PLA lattice samples (DNA and Hybrid) provide critical insights into their failure mechanisms and surface properties (see Figure 11). The fractured surfaces mostly exhibit brittle fracture characteristics, marked by sharp, uneven edges and a lack of substantial plastic deformation. The existence of micro voids and microcracks indicates areas of stress concentration that served as initiation points for cracks under load and certain regions, layered morphology and striations are evident, indicating the layer-by-layer nature of the SLA fabrication process and possible interfacial weaknesses between layers. Pull-out features and interfacial delamination observed in some micrographs suggest incomplete bonding between successive layers, contributing to early crack propagation.

Additionally, resin-rich zones and fused particle remnants were detected, especially around the fractured edges. These indicate possible thermal inconsistencies or excess resin accumulation during the printing or post-curing stages. The absence of shear yielding patterns further reinforces the dominance of brittle failure, in line with the material characteristics of SLA-cured PLA.

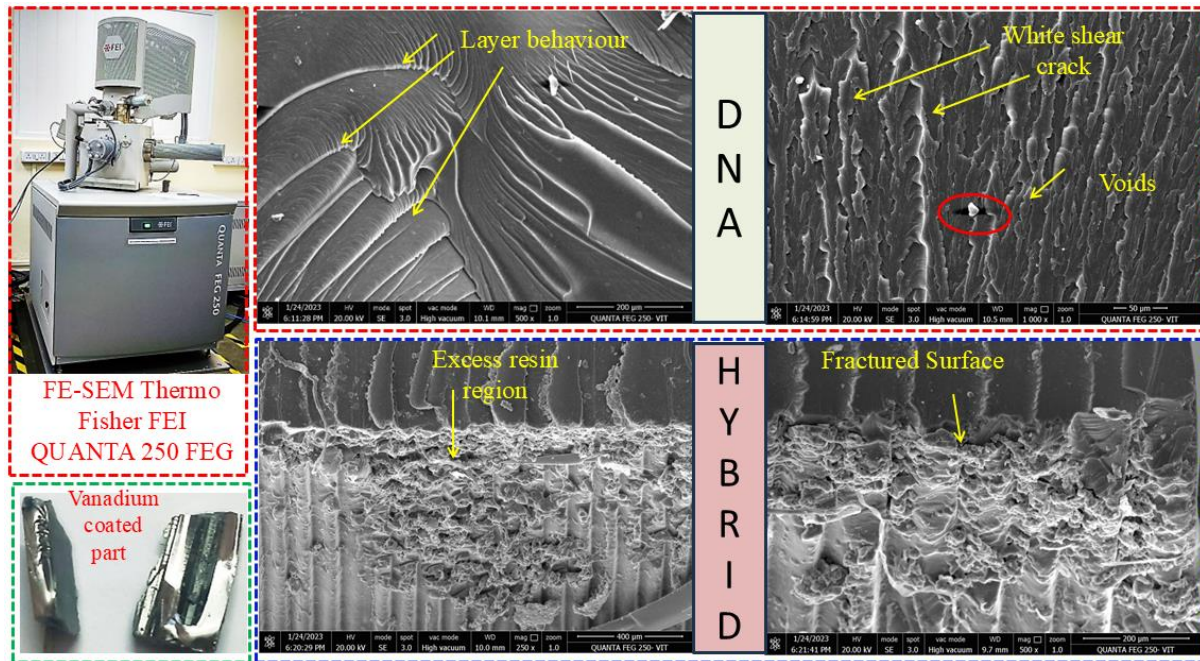


Figure 11 SEM analysis for fractured surface of DNA and Hybrid structure.

The fracture surface revealed minor defects, including voids and microcracks. To quantify the defect area, ImageJ software was employed to analyse the SEM images. The measured sizes of voids and cracks were approximately 44.28 μm , 65.70 μm , 48.97 μm , and 5.69 μm . The total calculated defect area constituted only 0.337% of the analysed surface, indicating a minimal presence of imperfections. This low defect fraction suggests that the overall mechanical performance of the SLA-printed ABS-like resin structures remains largely unaffected by these minor flaws.

Conclusion:

In this research, added two unique designs (DNA and Hybrid) to extend our previous work in which of three bio-inspired structures (Centriole, Nautilus, and Cartwheel) was developed and printed using the SLA 3d printing approach. This study systematically investigates and compares the compressive strength of two bio-inspired structures with previously developed configurations. The combination of DNA and cartwheel lattice structure offers average loading capacity and compressive strength in light weight category than previous work lattice structures.

- DNA structures exhibit low compressive strength due to their lean configuration; however, they demonstrate high strain values. Such elastic structures can be utilized in lightweight applications where limited strength is required.
- DNA structure used 45% and hybrid 24% less material than cartwheel structures.

- Hexagonal DNA lattice structures are challenging to manufacture due to the thin base pair dimensions, with some structures sustaining damage during removal from the platform.
- In comparison to the actual density, the average comparative density of samples is 10.2% lower.
- Hybrid structure with 0.9 mm thickness shown good compressive and energy absorption results.
- In the hybrid structure, the advantages associated with centriole and nautilus geometries were not effectively manifested.
- Compared to the centriole, nautilus, and previously reported hybrid structures, the DNA-based designs exhibit lower compressive strength. However, due to their characteristic deformation behavior, DNA structures show potential for use in energy-absorbing components, where controlled failure and flexibility are desirable.

Exploring alternative materials with higher ductility is proposed as a key direction for In future studies, the use of flexible or elastomeric materials will be explored to enhance the ductility and energy absorption capacity of DNA-inspired lattice structures. The current use of ABS-like resin provides good strength, but incorporating more deformable materials could lead to improved crashworthiness and resilience. Additionally, the effect of geometrical scaling, including variations in overall size, wall thickness, and unit cell dimensions, will be examined to optimize strength-to-weight ratios. A wider range of tube angles, beyond the current 35° and 40°, will also be investigated to better understand their influence on mechanical behavior, stress distribution, and failure mechanisms. Furthermore, modifications in DNA pattern designs, such as curvature, spacing, and interlink complexity, may lead to novel deformation modes and improved performance. The introduction of twisted or helical tube geometries is another promising direction, potentially enhancing torsional strength and energy dissipation, inspired by natural load-adaptive structures. These future developments aim to refine the balance between mechanical efficiency, manufacturability, and functional adaptability in bioinspired lattice systems.

Acknowledgement

For the purpose of open access, the author has applied a Creative Commons Attribution (CC BY) license to any Author Accepted Manuscript version arising from this submission”

Availability of data and materials

On request, the corresponding authors will provide all information and materials necessary to produce the findings in this study.

Declarations

Ethical approval: Not applicable.

Competing interests: The authors declare no competing interests.

Clinical trial number: Not applicable

References

1. Chouhan G, Gunji B, Bidare P, et al (2023) Experimental and Numerical Investigation of 3D Printed Bio-inspired Lattice Structures for Mechanical Behaviour Under Quasi Static Loading Conditions. *Mater Today Commun* 105658. <https://doi.org/10.1016/J.MTCOMM.2023.105658>
2. Liu L, Li L, Guo C, et al (2023) A Study of the Mechanical Properties of Naturally-Inspired Tubular Structures Designed for Lightweight Applications. *Appl. Sci.* 13
3. Dong B, Jia Y, Wang W (2025) Designing Load-Bearing Bio-Inspired Materials for Simultaneous Static Properties and Dynamic Damping: Multi-Objective Optimization for Micro-Structure. *Chinese J Mech Eng* 38:8. <https://doi.org/10.1186/s10033-024-01169-4>
4. Hössinger-Kalteis A, Lackner M, Major Z, et al (2024) Design method for individualised 3D printed lattice shoe midsoles. *Proc Inst Mech Eng Part L J Mater Des Appl* 14644207241291232. <https://doi.org/10.1177/14644207241291232>
5. Song S, Xiong C, Yin J, et al (2023) Failure mechanism and size effect of new bioinspired sandwich under quasi-static load. *Compos Struct* 324:117552. <https://doi.org/https://doi.org/10.1016/j.compstruct.2023.117552>
6. Sun Z, Gong Y, Bian Z, et al (2024) Mechanical properties of bionic lattice and its hybrid structures based on the microstructural design of pomelo peel. *Thin-Walled Struct* 198:111715. <https://doi.org/https://doi.org/10.1016/j.tws.2024.111715>
7. Yang B, Chen W, Xin R, et al (2022) Pomelo Peel-Inspired 3D-Printed Porous Structure for Efficient Absorption of Compressive Strain Energy. *J Bionic Eng* 19:448–457. <https://doi.org/10.1007/s42235-021-00145-1>
8. Wang E, Zhou J, Guo X, et al (2023) Numerical and constitutive modeling of quasi-static and dynamic mechanical behavior in graded additively manufactured lattice structures. *Virtual Phys Prototyp* 18:e2283027. <https://doi.org/10.1080/17452759.2023.2283027>
9. Yang H, Cao X, Zhang Y, Li Y (2024) 3D-printed bioinspired cage lattices with defect-tolerant mechanical properties. *Addit Manuf* 82:104036. <https://doi.org/https://doi.org/10.1016/j.addma.2024.104036>
10. Ramakrishnan R, Hemanth Kumar J, Titus F, et al (2024) Experimental investigation of 3D printed bio-inspired Xylotus lattice structure for energy absorption under quasi-static axial loading conditions. *Proc Inst Mech Eng Part L J Mater Des Appl* 238:1942–1955. <https://doi.org/10.1177/14644207241236856>
11. Guo Z, Yang F, Li L, Wu J (2024) Bio-Inspired Curved-Elliptical Lattice Structures for Enhanced Mechanical Performance and Deformation Stability. *Materials (Basel)*.

12. Mancini E, Utzeri M, Farotti E, et al (2024) DLP printed 3D gyroid structure: Mechanical response at meso and macro scale. *Mech Mater* 192:104970. <https://doi.org/https://doi.org/10.1016/j.mechmat.2024.104970>
13. Shirzad M, Kang J, Kim G, et al (2024) Bioinspired 3D-Printed Auxetic Structures with Enhanced Fatigue Behavior. *Adv Eng Mater* 26:. <https://doi.org/10.1002/adem.202302036>
14. Chouhan G, Bidare P (2024) Manufacturability of A20X printed lattice heat sinks. *Prog Addit Manuf*. <https://doi.org/10.1007/s40964-024-00923-3>
15. Munyensanga Patrick, Eddahchouri Hamza, Lamnawar Khalid, et al (2024) Lattice structures with a negative Poisson's ratio: Energy absorption assessment. *Cell Polym* 43:17–34. <https://doi.org/10.1177/02624893241232380>
16. AlQaydi HA, Krishnan K, Oyebanji J, et al (2022) Hybridisation of AlSi10Mg lattice structures for engineered mechanical performance. *Addit Manuf* 57:102935. <https://doi.org/https://doi.org/10.1016/j.addma.2022.102935>
17. Wang Z, Xu M, Du J, Jin Y (2024) Experimental and Numerical Investigation of Polymer-Based 3D-Printed Lattice Structures with Largely Tunable Mechanical Properties Based on Triply Periodic Minimal Surface. *Polymers (Basel)*. 16
18. Nazir A, Hussain S, Ali HM, Waqar S (2024) Design and mechanical performance of nature-inspired novel hybrid triply periodic minimal surface lattice structures fabricated using material extrusion. *Mater Today Commun* 38:108349. <https://doi.org/https://doi.org/10.1016/j.mtcomm.2024.108349>
19. Dutta H, Veeman D, Vellaisamy M (2024) Additively manufactured polymethyl methacrylate lattice structures: Effect of 3D hybridization on compressive strength. *Mater Lett* 377:137487. <https://doi.org/https://doi.org/10.1016/j.matlet.2024.137487>
20. Di Frisco G, Yousefi Nooraie R, Guagliano M, Bagherifard S (2024) Structural design and characterization of hybrid hierarchical lattice structures based on sheet-network Triply periodic Minimal surface topology. *Mater Des* 246:113336. <https://doi.org/https://doi.org/10.1016/j.matdes.2024.113336>
21. Minchin S, Lodge J (2019) Understanding biochemistry: structure and function of nucleic acids. *Essays Biochem* 63:433–456. <https://doi.org/10.1042/EBC20180038>
22. Fonseca Guerra C, Bickelhaupt FM, Snijders JG, Baerends EJ (2000) Hydrogen Bonding in DNA Base Pairs: Reconciliation of Theory and Experiment. *J Am Chem Soc* 122:4117–4128. <https://doi.org/10.1021/ja993262d>
23. Watson JD, Baker TA, Bell SP, et al (2013) *Molecular Biology of the Gene* (7th Edition). Pearson Education
24. Pray LA (2013) Discovery of DNA Structure and Function: Watson and Crick. In: *Nature Education*. p 1(1):100
25. Ghannam JY, Wang J, Jan A (2025) *Biochemistry, DNA Structure*. StatPearls Publishing, Treasure Island (FL)